

This item is the archived peer-reviewed author-version of:

Some critical observations about the degradation of glass : the formation of lamellae explained

Reference:

Schalm Olivier, Nuyts Gert, Janssens Koen.- Some critical observations about the degradation of glass : the formation of lamellae explained
Journal of non-crystalline solids - ISSN 0022-3093 - 569(2021), 120984
Full text (Publisher's DOI): <https://doi.org/10.1016/J.JNONCRY SOL.2021.120984>
To cite this reference: <https://hdl.handle.net/10067/1798350151162165141>

Some critical observations about the degradation of glass: the formation of lamellae explained

Olivier Schalm ^{a,b,*}, Gert Nuyts ^c, Koen Janssens ^c

a. Antwerp Maritime Academy, Noordkasteel Oost 6, 2030 Antwerpen, email: olivier.schalm@hzs.be

b. University of Antwerp, Conservation Studies, Blindestraat 9, B-2000 Antwerp, Belgium

c. University of Antwerp, Department of Chemistry, Groenenborgerlaan 171, B-2020 Antwerp, Belgium

Keywords: glass, degradation, mechanism, lamellae, internal structure

Abstract

This study demonstrates that the mechanism responsible for the transformation of glass into a degradation layer is pH-dependent. In acid conditions, the transformed glass is homogeneous and brittle. In mild alkaline conditions, transformed glass is heterogeneous due to the presence of lamellae composed of silica nanoparticles and the occurrence of Ca-rich inclusions. The fundamental difference between acid and alkaline conditions cannot be explained by the currently accepted degradation mechanism based on ion exchange. To explain this critical observation, we propose a refined degradation mechanism based on existing knowledge that involves several inwardly moving reaction fronts. The fronts responsible for the transformation of the silicate network into amorphous silica are also responsible for the morphology of the transformed glass. We have identified the feedback mechanism that explains the formation of lamellae in alkaline conditions.

1. Introduction

Historical glass showing signs of degradation can usually be described as a combination of 3 phases: (1) the remaining healthy glass, (2) a silica rich layer depleted from its mobile cations (such as Na^+ , K^+ , Mg^{2+} and Ca^{2+}), and (3) the weathering crust on top of the (original) material surface. These phases are typically separated by sharp boundaries. In some cases, pits can be found at the level of the material surface [1]. There is a various and confusing terminology used in the literature to describe the degraded zone just beneath the surface [2]. Probably, the most confusing term is 'diffusion layer', which is either used to denote the complete layer of degraded glass through which reagents are transported or the layer formed during the ion exchange process. To avoid confusion for the reader, throughout the remainder of the manuscript the more neutral term 'transformed glass' will be used for the degraded zone. Similarly, the degradation process leading to transformed glass will be denoted with the term 'transformation process'. The transformed glass usually is considered as a homogeneous silica-rich material. However, transformed glass is often extremely heterogeneous. Examples of such heterogeneities in transformed glass are the existence of lamellae, the preferential occurrence of Mn-rich inclusions in the darker lamellae, Mn-rich dendrites or Mn-rich nodules, the formation of insoluble salts such as calcium carbonates or phosphates or even the penetration of cations such as Pb^{2+} from the environment [3, 4, 5]. From all these phenomena, the occurrence of silica nanoparticles and the formation of lamellae are critical features that must be explained by the transformation mechanism itself. The other phenomena leading to heterogeneities can be explained by processes that occur within the transformed layer (i.e., the transformed layer must be formed first).

There is literature that specifically deals with lamellae in transformed glass. Brewster mentioned the presence of lamellae on wine bottles brought up from the 'Royal George' [6]. Guillot performed

experiments to generate lamellar transformed glass using saturated NaHCO_3 solutions [7], while Roemich et al. introduced $(\text{NH}_4)_2\text{CO}_3$ in soil experiments to adjust the pH [8]. The mentioned experiments suggest that lamellae are formed under alkaline conditions. They are formed in static conditions and cannot be explained by external cyclic (e.g., seasonal) fluctuations as was suggested by Brill [9]. The seasonal changes at the bottom of the sea must be too small to be the driving force for the formation of lamellae in marine conditions [10, 11]. Several authors reported the presence of lamellae in land-based and in marine conditions [12, 13], suggesting that lamellae are formed in different kinds of environmental conditions.

The most commonly accepted description of the transformation process is based on an ion exchange process where protons from the bulk solution surrounding the glass enters the silicate network, leaching out the mobile cations [14]. This is in agreement with experiments in acid solutions where ion exchange proceeds rapidly at low pH and slows down as the pH rises. The pH of the bulk solution increases with the square root of time for short-term experiments, a typical property of diffusion processes [15, 16]. The weathering crust formed on the (original) glass surface is the result of the precipitation of leached cations when the water at the glass surface evaporates. Crusts on historical stained glass windows are mainly composed of sulphates [17, 18, 19]. When the pH exceeds 9-10, the dissolution of the silica network becomes the dominant process. The above indicates that the transformation mechanism of glass is pH-dependent. At locations where the solution is not regularly replenished the accumulation of OH^- ions in the water leads to an increase in the pH value, resulting in the formation of pits in the glass surface [20]. However, silica chemistry is more complex than the commonly accepted transformation suggests and it is also pH dependent. The work of Iler shows that monosilicic solutions turn into a homogeneous gel in acid conditions but lead to the formation of particles in alkaline conditions [21]. Several recipes exist to produce silica nanoparticles in alkaline solutions [22, 23, 24, 25, 26, 27]. Materials composed of amorphous silica nanoparticles also exist in nature (i.e., opals) [28, 29, 30, 31]. Recently, we reported that the differences between subsequent lamellae is mainly caused by a packing difference in amorphous silica nanoparticles: random loose packing (RLP) and random close packing (RCP) [2]. This contribution will demonstrate that the morphology of transformed glass is pH dependent and that the presence of nanoparticles and lamellae are formed under static, alkaline conditions. The formation of lamellae suggests the presence of a feedback loop in alkaline conditions that apparently does not exist in acid conditions. These are critical observations that need to be incorporated in the description of the transformation mechanism.

The existence of lamellae in the transformed glass and the resulting phenomenon of iridescence were one of the main reasons why the attention of scientists at the end of the 19th century was attracted by the degradation of glass [6]. It is surprising that from the mid-20th century onwards the formation of lamellae appears to be neglected or overlooked in most of the degradation-related literature. In addition, the occurrence of lamellae is an often occurring phenomenon in the case of archaeological glass [32, 33, 34, 35, 36, 37, 38, 39, 40, 41] but is only rarely reported in glass degradation experiments in laboratory conditions [7, 8]. It should be remarked that the occurrence of a (nanometer-) sharp interface between healthy glass and transformed glass [42] is not in agreement with the typical interdiffusion profiles that are expected from Fick's law. In addition, the diffusion process is not able to explain the transformation of the silicate network into amorphous silica, to explain the formation of silica nanoparticles and the formation of lamellae. An alternative mechanism involves a set of interacting reactions such as hydration, dissolution, condensation/precipitation and ion

exchange/interdiffusion [43, 44]. Such models can be considered as Petri nets where all reactions occur simultaneously in a homogeneous medium and each reaction influences the kinetics of the other reactions [45]. This model can explain temporal evolutions such as the transformation of the original silicate structure resulting in amorphous silica [46, 47], the uptake of oxygen isotopes from the bulk solution by the silica structure [43], the increase in pH [48], and/or the ripening of transformed glass over time [49]. However, it is not able to explain spatiotemporal dynamics. The occurrence of lamellae is sometimes explained as Liesegang bands where precipitation reactions are coupled to transportation mechanisms. Liesegang bands are a well-known example of spatiotemporal self-organization [7, 32, 50]. If lamellae would be Liesegang bands, then the lamellae are supposed to have a chemical contrast. This idea is in agreement with some samples showing alternating darker (i.e., rich in MnO_2) and brighter bands (i.e., poor in MnO_2) [51] or where layers with compositional differences in Al/Si or Ca/P can be seen [5, 10, 36, 41]. However, alternating bands are also observed in the absence of chemical contrasts [2]. In addition, a Liesegang mechanism is not able to explain the formation of silica nanoparticles that make up the lamellae. An alternative explanation is that cracks separate the consecutive lamellae but one can question how the lamellae are held together [52, 53]. Newton suggests that there should be a mechanism which returns the reaction conditions to some previous state [11]. However, Newton ends his conclusion with the following sentence: "I cannot as a glass technologist yet say with any conviction how any of the layers get there!" Also Cox and Ford suggested that the transformation mechanism can change the reaction conditions periodically, which affects the precipitation of secondary products [54]. The mentioned theories make it clear that the currently accepted transformation mechanisms must be considered as incomplete.

A recently proposed transformation mechanism combines the transportation mechanisms with the interplay of chemical reactions. It assumes the existence of 2 inwardly moving reaction fronts in a zone between the healthy glass and transformed glass: (1) an ion exchange process, followed by (2) an interface coupled dissolution-precipitation (ICDP) front that transforms the leached silicate skeleton into amorphous silica [42, 50, 55, 56, 57, 58, 59]. The literature about that model suggests the existence of a feedback mechanism but it is only described superficially [55, 60]. We propose a refined version of the latest transformation mechanism explaining several critical observation such as the pH-dependency of the transformation mechanism or the formation of silica nanoparticles resulting in lamellae.

2. Experimental

2.1. Degradation experiments

Two model glass types MI and MIII, purchased from the Fraunhofer Institut für Silicatforschung in Würzburg, Germany were used in degradation experiments. The compositions of both glass types are given in Table I. Glass type MI corresponds with a typical medieval potash with a SiO_2 content lower than 50 w%; while glass type MIII is a typical 16-17th century potash glass with a SiO_2 content higher than 50 w% [61, 62]. The surface of the samples were fired polished. The thickness of the glass slides was 0.7 mm. Both glass types are potassium-rich glass and are more sensitive towards degradation when compared to modern sodium-rich glass compositions so that the experiments yielded faster results. The degradation experiments were performed with the more sensitive MI glass (i.e., containing less SiO_2) and the more stable MIII glass (i.e., containing a higher SiO_2 content) glass type.

TABLE I: Chemical composition of the model glass types used in the degradation experiments (values expressed in wt%) [61].

Glass type	Na ₂ O	MgO	Al ₂ O ₃	SiO ₂	P ₂ O ₅	K ₂ O	CaO
MI	3.0	3.0	1.5	48.0	4.0	25.5	15.0
MIII	0	0	0	60.0	0	15.0	25.0

A series of experiments were performed in Duran bottles with a small neck. A small hole was drilled in the centre of the caps. A nylon wire was pulled through the hole and fixed on the outer side of the caps using glue (the latter was applied with a hot glue gun, closing the hole). A glass fragment was attached to the end of the nylon wire using a hot glue gun so that the glass fragment could be suspended in the centre of the solution. The temperature of the solutions was about 22°C. The following parameters were varied to explore their impact on the formation of nanoparticles and lamellae (see Table II).

- **Glass type:** Two glass types were used in the experiments. For the MIII type glass fragments, only experiments in solutions with initial pH 1.5, with and without stirring were performed.
- **Bulk solution:** Degradation experiments were performed in acid conditions (i.e., HCl solution of pH 1.5 or 5.8), in distilled water (pH = 7) and in saturated NaHCO₃ solutions (pH = 8.3). Solutions were prepared by diluting Titrisol HCl (1000 mL, 0.1 mol/L) to obtain the required pH and by dissolving NaHCO₃ in order to obtain a saturated solution.
- **Exposure time:** Exposure times ranged from 14 days for the highly acidic solutions until almost 2 years for the alkaline solutions.
- **Volume of the bulk solution:** Some experiments were performed in smaller bottles to vary the volume of the bulk solution. Experiment 8 was performed in a sputum bottle and experiment 9 in an Eppendorf tube
- **Homogenization:** In some experiments, the bulk solution was homogenized with a magnetic stirrer. In other experiments, concentration gradients were allowed to form spontaneously in the solution.

TABLE II: Overview of the experimental conditions. The average degradation rate determined by the thickness of the transformed glass and the exposure time is not reported because the rate slows down over time as the pH of the solution increases. For long exposure times, the transformation rate is misleading low.

Nr.	Glass type	Solution	Volume (mL)	Homogenization	Mass glass (g)	Total surface area (mm ²)	Initial pH	pH end	Exposure time (days)	Lamellae
1	MI	HCl	250	Yes	0.281	287	1.5	1.7	14	No
2	MI	HCl	250	No	0.263	285	1.5	1.9	14	No
3	MIII	HCl	250	Yes	0.308	347	1.5	1.8	14	No
4	MIII	HCl	250	No	0.314	372	1.5	1.7	14	No
5	MI	Saturated NaHCO ₃	250	No	0.153	158	8.4	10	70	Yes
6	MI	Saturated NaHCO ₃	250	No	0.151	166	8.3	10	712	Low contrast
7	MI	Saturated NaHCO ₃	250	Yes	0.198	201	8.22	8.7	748	Yes
8	MI	Saturated NaHCO ₃	10	No	0.122	147	8.2	10.5	101	Low contrast
9	MI	H ₂ O	1	No	0.089	89	7	c. 10	101	No
10	MI	H ₂ O	250	No	0.173	172	7	8.79	712	Yes

11	MI	HCl	250	No	0.498	193	5.8	8.05	712	Low contrast
----	----	-----	-----	----	-------	-----	-----	------	-----	--------------

2.2. Material characterization

Some of the samples were analyzed from their polished cross-section. The preparation of these samples is described elsewhere [2]. Since the polishing process can modify the morphology of the internal structure, the cross-section was also studied by breaking a small fragment of the treated glass fragment using a pair of tweezers. The chip was positioned vertically in the scanning electron microscope (SEM) so that the cross-section could be analyzed. For this, the sample was attached to the SEM sample holder using plasticine. Prior to analysis, the polished samples and the freshly broken surfaces were carbon coated.

The surfaces were examined with a Field Emission Gun – Environmental Scanning Electron Microscope (FEG-ESEM) equipped with an Energy Dispersive X-Ray (EDX) detector (FEI Quanta 250, USA; at the AXES and EMAT research groups, University of Antwerp). The measuring conditions were an accelerating voltage of 20kV, a take-off angle of 30°, a working distance of 10 mm and a sample chamber pressure of 10^{-4} Pa. Images were collected in backscattered electron mode in order to obtain a maximum contrast between the lamellae. Secondary electron images were collected to study the surface morphology. For both imaging modes a beam current of ca. 0.8 nA was used.

3. Results

The series of experiments described in Table I provide an overview of the parameters that have been varied. From a visual point of view, all experiments resulted in an opaque and fragile surface. None of the samples generated the typical iridescence colours. There is no obvious visual difference in the appearance of the transformed layers between the experiments in acid and alkaline conditions. When considering the average transformation speed in $\mu\text{m}/\text{day}$, the acidic conditions (i.e., experiment 1 and 2 show a transformation speed higher than $2 \mu\text{m}/\text{day}$) are more aggressive than alkaline conditions (experiment 5, 6 and 7 show a transformation speed below $1 \mu\text{m}/\text{day}$). It should be noted that the degradation rate is initially high and that it slows down over time. It explains why the degradation rate of experiment 5 (exposure time: 70 days and $1 \mu\text{m}/\text{day}$) is higher than the ones of 6 and 7 (exposure time: more than 700 days and below $0.2 \mu\text{m}/\text{day}$) while the initial degradation conditions are the same. The transformation speed depends on the concentration of available protons in the bulk solution. This means that the transformation in alkaline conditions occur at a slower speed. It suggests that the rate determining factor of the overall transformation process in bulk solutions at pH below 10 is the ion exchange process. At pH above 9-10, the dissolution of the silicate network becomes the rate-controlling reaction front. Table I suggests that lamellae are formed in a broad range of conditions as long as the environment is in the alkaline pH-range, although the contrast between subsequent lamellae can be variable. In the following sections, the results of some of the experiments will be described in more detail. A distinction is made between several environmental conditions.

3.1. Experiments in acid conditions

The final pH at the end of experiments 1 to 4 were all below 7, i.e., the complete transformation process was performed in acidic conditions (see Table I). The transformed glass of the MIII glass (i.e., experiment 3 and 4) had a thickness of about $15 \mu\text{m}$. The transformation rate of MIII was considered

too low for further studies. For that reason, the MIll glass was omitted from the experiments in alkaline solutions. However, archaeological glass studies revealed that lamellae are also formed on this glass type and even on soda-lime glass [62]. This suggests that the chemical composition is not a determining factor for the absence or presence of lamellae. For MI glass, the polished cross-sections showed the presence of transformed glass on both sides of the sample. The thickness was about 300 μm . Stirring did not seem to affect the transformation speed. Inside the transformed glass, there were no internal features to be seen except for cracks. To avoid the detrimental effect of polishing on the morphology of transformed glass, a fragment from experiment 1 was broken off and observed microscopically (Fig. 1). Only a thin layer of healthy glass remains at the position of the arrow in Fig. 1b. The interface between transformed layer and healthy glass is a sharp step-like profile. This observation is not in agreement with a diffusion process. The BSE images obtained at different magnifications (Figs. 1b, c and d) suggest that the transformed glass is homogeneous at the microscopic level. The transformed glass is brittle, showing Wallner lines (i.e., a distinct pattern of intersecting sets of parallel lines as in Fig. 1d).

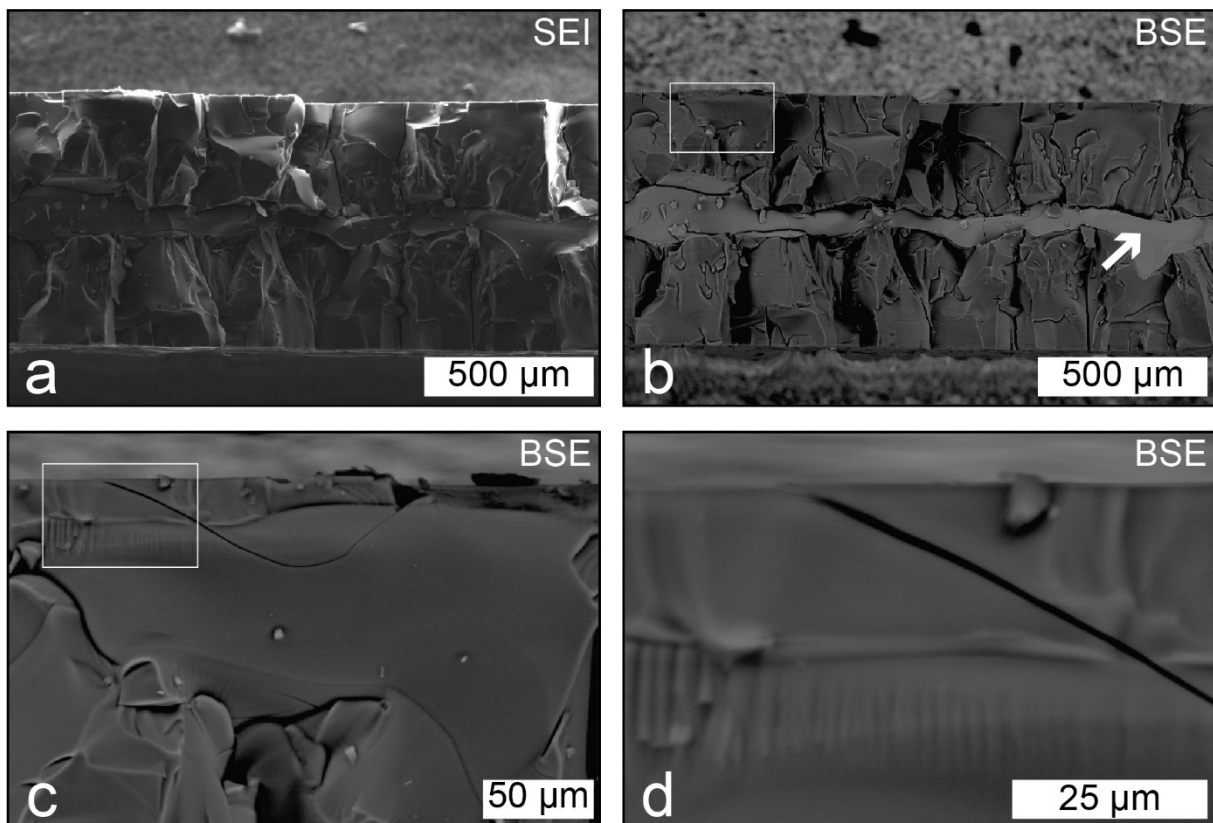


Fig. 1: Cross-sectioned sample from experiment 1 obtained by breaking. Some remaining healthy glass is seen in the centre (arrow) while transformed glass is present at both sides. a) Secondary electron image at low magnification; b) backscattered electron image of the same position as image a; c) backscattered electron image of the rectangle in image 1b in b; d) backscattered electron image of the rectangle in image 1c.

3.2. Experiments with a transition from acid to alkaline conditions

In experiment 11, the initial pH of the HCl-solution was 6 but it evolved to 8.05. This means that the experiment evolved from acidic towards alkaline conditions. Observations showed that the

transformed glass consisted of 3 zones: (1) a zone close at the original outer surface where no lamellae could be observed that is formed at the start of the experiment, (2) a zone that is rich in Ca, and (3) a zone closer at the inner surface where lamellae are present but where the BSE contrast between lamellae is small. The zone closer to the healthy glass is formed at the end of the experiment and thus in alkaline conditions. A limited contrast between lamellae has been reported earlier [2]. X-ray spectra of the Ca-rich zone indicates the presence of O, Si and Ca. This experiment suggests that the degradation mechanism above and below the Ca-rich zone is different. Moreover, the BSE contrast between lamellae appears to change from sample to sample.

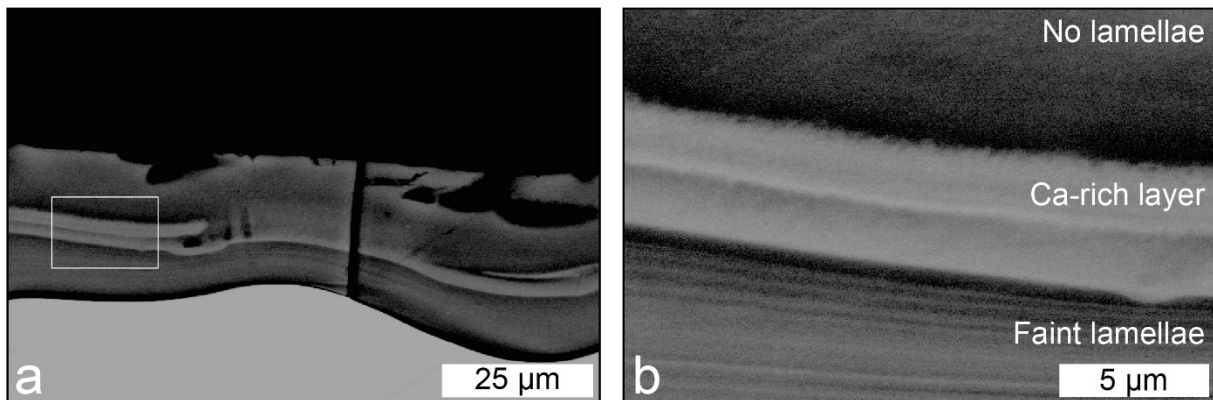


Fig. 2: Polished cross-section of the glass resulting from experiment 11 during which the mild acidic conditions evolved towards alkaline conditions. The transformed glass close to the outer surface was formed in acidic conditions and the transformed glass close to the inner surface was formed in alkaline conditions. a) Overview of the sample; b) Detail of the transformed glass showing the transition in the transformation mechanism.

3.2. Experiments from neutral to alkaline conditions

In experiment 10, the MI-glass was immersed in distilled water (pH = 7) for a period of 712 days. The solution gradually evolved towards alkaline conditions: the pH of the solution increased up to 8.79 ($\Delta\text{pH} = 1.79$). In Fig. 3a and b, an overview from a polished cross-section is presented in BSE mode. The transformed glass has a thickness between 230 μm and 300 μm . The inner surface (interface at the healthy glass) appears to be very sharp while the transformed glass contains low-density and high-density lamellae with a clear contrast. Even at the surface, lamellae can be observed, suggesting that in solutions of pH 7 lamellae are formed. This demonstrates that in laboratory conditions transformed glass composed of lamellae can be formed. The grey values of the BSE image along the dotted line shown in Fig. 3b are plotted in Fig. 3c. On a distance of 120 μm , 63 well defined maxima are identified. Since the valleys of that profile are associated with low density lamellae, 126 lamellae are present on that distance, indicating that the lamellae have an average thickness of about 1 μm . Since the thickness of the lamellae is substantially larger than the wavelength of visible light, they cannot cause interference and thus this sample does not show iridescence. It should be remarked that the fluctuations in grey value in Fig. 3c are quasi-periodical, suggesting that the effective thickness of the lamellae around the average of 1 μm varies randomly. This means that the reaction conditions responsible for the transition from a high-density lamella to and low-density lamella occur at unpredictable moments.

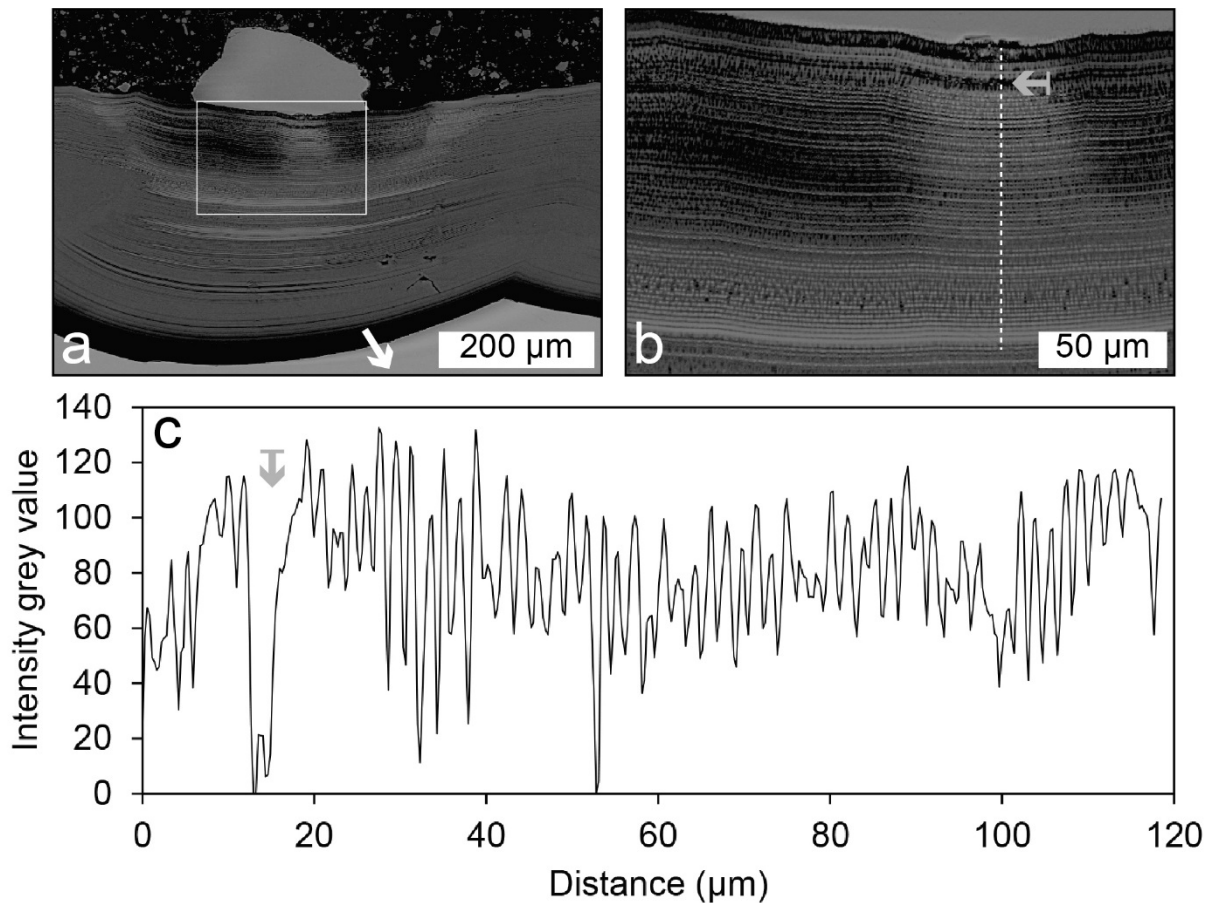


Fig. 3: Polished cross-sectioned sample obtained from experiment 10. a) Overview of the sample in BSE mode; b) Close up in BSE mode visualizing the lamellar structure of transformed glass; c) Grey value intensity along the line shown in Fig. 3b perpendicular to the lamellae. The distance at 0 μm corresponds with the position of the outer surface. The grey arrow corresponds with the dark zone.

From the same experiment 10, a broken-off surface was analysed as well. The SEI and BSE images in Fig. 4a and b show the presence of features organized along lines. In this sample, the contrast between the subsequent lamellae is weak compared to the polished sample in Fig. 3. At higher magnifications the presence of nanoparticles of c. 100 nm and smaller can be seen. The nanoparticles are clearly visible in SEI; in BSE mode this information is lost. This experiment demonstrates that it is possible to generate transformed glass composed of nanoparticles in a static solution. Fig. 4c suggests that the presence of lamellae is related to the formation of nanoparticles. Moreover, the morphology of transformed glass is clearly different from the sample immersed in an acid solution (see Fig. 1).

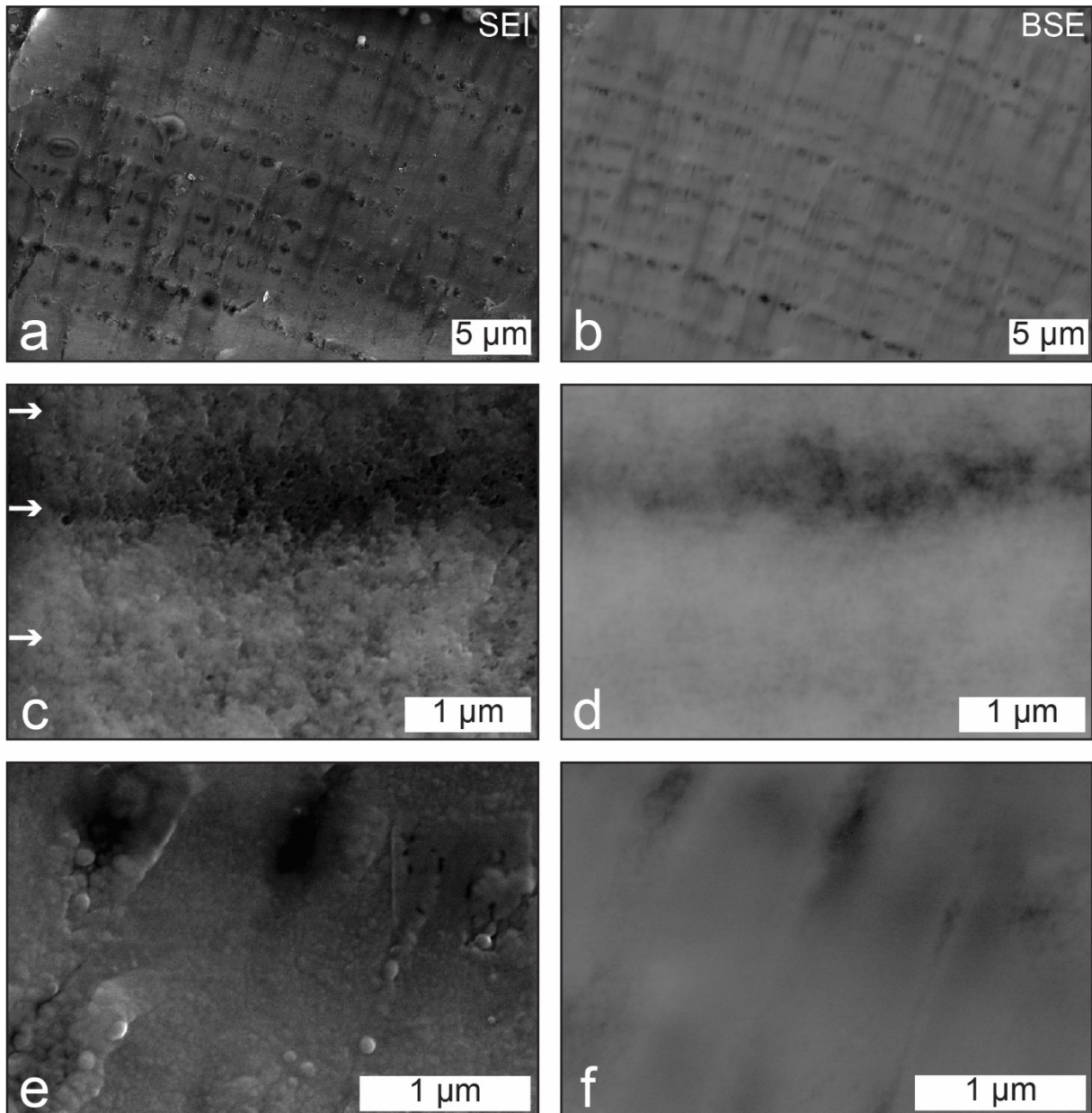


Fig. 4: Cross-sectioned sample from experiment 10 obtained by breaking off a piece of the treated glass without additional sample preparation. The images on the left are secondary electron images (SEI) while the images at the right are backscattered electron images (BSE); a and b) overview of the sample with pores organized along lines; c and d) Detail of several lamellae as indicated by the arrows; e and f) High magnification image of the transformed glass showing the presence of nanoparticles.

3.3. Experiments in alkaline conditions

Experiments 5 to 8 are performed in saturated NaHCO_3 solutions in order to repeat the reported experiments of Guillot [7]. The initial pH was about 8.2 and evolved towards a value of 10. All NaHCO_3 -experiments resulted in lamellae, although the observed contrast between the lamellae varies. A remarkable feature is that inside the transformed glass Ca-rich nodules are encountered, a phenomenon that was not observed in acid conditions. This can be seen in Fig. 5. These nodules contain both Si and Ca and are enclosed by a sharp boundary. In the BSE-image, the contrast is caused by differences in mean atomic number (different amounts of Ca) and/or in average density (i.e., lamellae are mainly composed of SiO_2 , H_2O and voids and the packing density of silica nanoparticles between lamellae is different). In a previous report [2], it was stated that precipitates can be formed

in the voids between the silica nanoparticles. However, the explanation of Guillot that lamellae consists of alternating layers of silica-rich and Ca-rich layers is not in agreement with the analyses performed on the samples of experiments 5 to 8 and with the other experiments summarized in Table I.

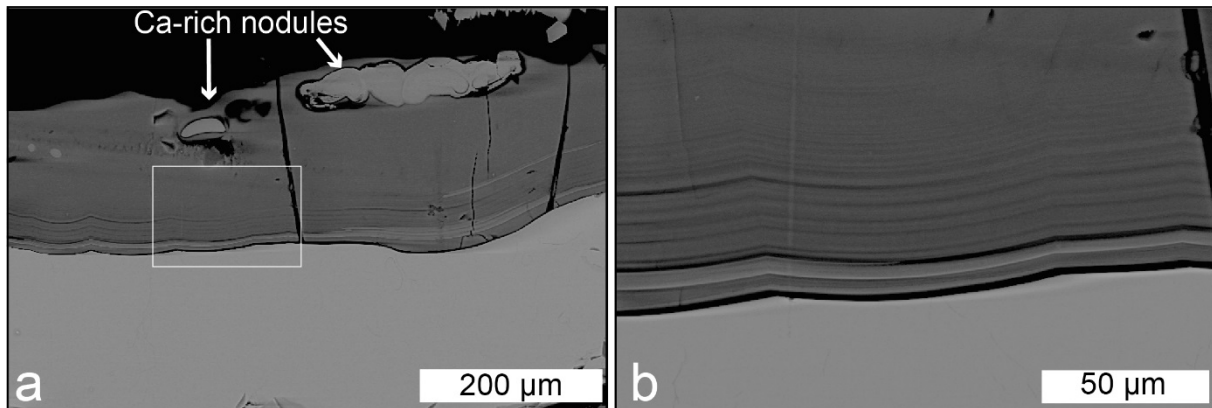


Fig. 5: A polished cross-sectioned sample obtained from experiment 7 using a saturated NaHCO_3 solution where Ca-rich nodules are observed in BSE mode and where the contrast between the lamellae is sufficiently high to visualize them. a) Overview of the sample; b) Detail visualizing the lamellae.

4. Discussions

The previous section demonstrated that transformed glass can be formed in acid and in alkaline conditions. It also showed that the same glass transforms in solid materials with different morphologies and that this process is affected by the pH. The generally accepted mechanism that is supposed to describe such transformations consists of several chemical processes [65, 66, 67, 68]: (1) a diffusion process that is responsible for the ion exchange between protons in solution and the mobile cations in the silicate network, (2) penetration of water molecules in the silicate network by permeation in the nanoporosity of the silicate network (i.e., a diffusion process) or by hydration and condensation reactions (i.e., diffusion-reaction mechanism [67, 68]) [69], (3) the reaction of hydroxyl ions in solution with the silicate network (i.e., hydrolysis), and (4) the reaction of extracted cations with atmospheric gases [70]. These processes are often presented as separate chemical reactions. Some authors state that these 'elementary chemical mechanisms' are strongly coupled [49] (as in a Petri net). Some make a distinction between 2 alteration mechanisms: interdiffusion and dissolution [71]. Others mention the existence of reaction fronts and interface reactions [54], a reaction zone (i.e., zone where glass surface sites interact with the ions in solutions) [72] or a diffusion control zone with a thin and constant thickness between unhydrated glass and hydrated glass within the glass [16] more explicitly. The presence of 2 reaction zones is sometimes reported as well: one at the outer surface and another one at the inner surface [15]. Information about the reactivity of silica in alkaline conditions can also be found in the literature about the degradation of cement where reactive silica is transforming into a gel through several sequential reactions. That sequence is known as the alkali-silica reaction mechanism and consists of: (1) dissolution of silica due to hydroxyl ions available in the pore solution, (2) formation of nano-colloidal silica sols, (3) gelation of the sols, and (4) swelling of the gel when absorbing water [75, 76, 77]. The series of moving reaction fronts can also be considered as sequential reactions.

The more recent transformation mechanisms relying on moving reaction fronts are summarized in Fig. 7. Such moving reaction fronts can easily explain how the transformation is influenced by irregularities

in the glass surface (e.g., surface roughness, surface defects such as scratches or pits) [71], leading to for example hemispherical reaction fronts (e.g., Fig. 3a). In the processes proposed in Fig. 6, the chemical reactions accepted by the heritage community are considered as localized chemical reactions (i.e., a specific type of solid-state reaction) [73] that occur at inwardly moving fronts. The transport of species couples the reaction fronts with each other. The mechanism that dominates the transformation process is determined by the pH of the local solution. The transformation mechanisms in Fig. 6a and 6c show the generally accepted mechanisms of the formation of transformed glass in acid conditions and the dissolution of glass in alkaline conditions. With Fig. 6b, we propose a new process with a feedback loop that explains the formation of transformed glass in alkaline conditions. Others have already suggested a process with a vaguely described feedback mechanism, but we propose that this process only occur in a mild alkaline pH range. That model assumes that transformed glass formed in alkaline solutions consists of lamellae composed of a random packing of silica nanoparticles as is observed in earlier work [2] and in this contribution.

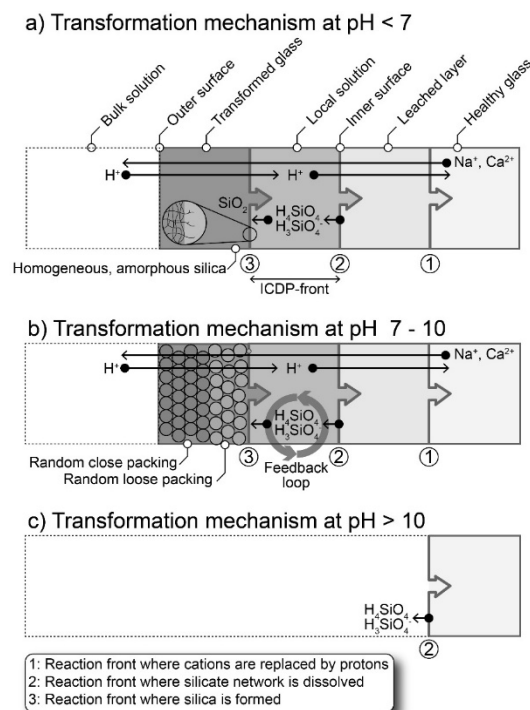


Fig. 6: Transformation mechanism of glass when immersed in solutions of different pH. The overview also visualizes the transport of species. a) Transformation mechanisms in acid solutions based on 2 inwardly moving reaction fronts: the ion-exchange process at reaction front 1 and the interface coupled dissolution-precipitation (ICDP) front consisting of the coupled fronts 2 and 3; b) Transformation mechanisms in mild alkaline conditions with the formation of nanoparticles and lamellae due to a feedback mechanism in the local solution; c) Transformation mechanism in high alkaline conditions.

Fig. 6 proposes that the transformation of glass is governed by 3 different mechanisms. Depending of the pH of the solution, one of these variants will be the dominant transformation mechanism. The mechanism shown in Fig. 6a occurs in acid conditions. The transformation rate is governed by reaction front 1 (i.e., the ion exchange process). Experiments have demonstrated that the mechanism of Fig. 6a causes an increase of the pH and that highly alkaline solutions (pH > 9-10) can be obtained. This means that the dominating mechanism of Fig. 6a will gradually drop in importance and that the mechanism in Fig. 6c will become the dominating mechanism. This shift explains the formation of pits at the glass surface when dissolution occurs in locally distinct spots as can occur on stained-glass windows in

ambient air [1]. In that mechanism, reaction front 2 (i.e., responsible for the dissolution of the silicate network) gradually takes over the role of rate limiting step [74]. The transition from homogeneous transformed glass to transformed glass with a lamellar structure as observed in Fig. 2 can be considered as an evolution from the mechanism of Fig. 6a to the one shown in Fig. 6b. This suggests the occurrence of different transformation mechanisms in different pH ranges. Before the transformation mechanisms of Fig. 6a and 6b are explained in detail, several concepts mentioned in Fig. 6 will be defined:

- **Outer surface:** This surface is the original glass surface and distinguishes the bulk solution from the solid material. On top of that surface, secondary corrosion products can precipitate, leading to a loss of transparency [75]. That phenomenon is especially important for transformation processes of stained-glass windows in ambient air;
- **Inner surface:** The inner surface is a sharp border between the solid material with the original silicate network (including the leached layer) and the silica solid where that network has been destroyed. The inner surface can be recognized as a sharp transition in cross-sectioned samples using microscopic techniques. The variable thickness of transformed glass as is often observed suggests that the outer surface does not displace (i.e., no dissolution of the glass, volume of transformed glass is identical to that of the original glass) but that the inner surface moves inwardly. For the mechanism shown in Fig. 6c the silicate material is dissolved so that the outer surface moves along with reaction front. For this mechanism, there is no inner surface;
- **Transformed glass:** This material is composed of amorphous silica and is depleted from the mobile cations. This layer has a nearly constant composition, independent of the network modifier concentration of the bulk glass [75]. Transformed glass is a different material when compared to the leached layer where the silicate skeleton remains. During the transformation process, reagents must diffuse through the growing layer of transformed glass before they reach the reaction fronts. In that sense, this 'diffusion layer' can slow down further transformation and act as a protective barrier. Within the transformed glass, different kinds of precipitates may be formed (e.g., Ca-rich precipitates in Fig. 6);
- **Leached layer:** The leached layer is located just below the inner surface. It is a small zone where cations are replaced by protons while the silicate network remains intact. The width of the hydrogen concentration gradient does not appear to be larger than 0.1 – 0.2 μm [76, 77, 78]. For that reason, that layer is not visible with microscopic techniques. In the literature [75], the term 'leached layer' is often used to denote 'transformed glass'. This is confusing because there are sufficient indications that the molecular structure of the silicate network endures a drastic change. Therefore, transformed glass should not be considered as a leached layer.
- **Local solution:** A thin fluid film separates the parent phase (i.e., the original silicate network that is dissolved at reaction front 2) and the product phase (i.e., transformed glass formed at reaction front 3). The local solution moves along with the ICDP front because at one side of the local solution (i.e., reaction front 2) the silicate network dissolves and at the other side of the local solution (i.e., reaction front 3) the open space is filled with precipitated silica. It has been shown that the physicochemical properties of the local solution differ from that of the bulk solution (such as pH) [42]. Since transformed glass is mechanically attached to the healthy glass, it is possible that the local solution is located in interconnected pockets. However, a gap up to 50 μm between leached layer and transformed glass has been reported [60]. When independent reaction fronts meet and coalesce, the solution of both fronts are homogenized

so that an identical reaction front is formed. From that point onwards, the individual lamellae remain in correct register [54].

- **ICDP-front:** The ICDP-front is the zone containing reaction front 2 and 3 with the local solution in between. The observations done in this study shows the crucial role of the ICDP-front because it is that front that determines the morphology of transformed glass. We propose a more detailed description of the transformation process that is able to explain the different morphologies and the formation of lamellae. The feedback loop responsible for the formation of lamellae takes place in the local solution (i.e., visualized as the circular arrows in Fig. 6b).

4.1. Transformation mechanism in acid conditions (pH < 7)

In acid conditions, transformed glass is formed through the mechanism shown in Fig. 6a. The rate at which this mechanism occurs is governed by the interdiffusion process of alkali and H^+ ions as described by Fick's laws [14, 15, 76, 79, 80]. The composition dependent diffusion coefficients explain why some glasses are more resistant against degradation. Reaction front 1 is responsible for the uptake of protons from the local solution (the fluid film between front 2 and 3 in Fig. 7). This results in a proton concentration gradient between local solution and bulk solution, setting up a migration of protons from the bulk solution towards the inner surface by diffusion through the transformed glass. This means that there is a diffusion process of protons through the growing layer of transformed glass and another diffusion process through the leached layer. During that process, the silicate network is supposed not to be involved in that process [81].

Reaction front 2 (i.e., dissolution of the leached silicate network) and front 3 (i.e., precipitation of dissolved silicic compounds as amorphous silica) constitutes the interface coupled dissolution-precipitation (ICDP) front and follows the slower but rate-limiting reaction front 1 at close distance [42, 56, 57]. The ICDP-front explains why the diffusion layer at front 1 remains small at all moments and why the inner surface has a sharp boundary (i.e., an atypical property for a diffusion process). The transformation of the original silicate network towards a structure closer to that of silica glass also occurs in extreme acid solutions such as in concentrated boiling sulphuric acid [82, 83]. This transition has been observed with FTIR analyses [46, 47, 63, 89, 90] and Raman analyses [87, 88]. This means that the ICDP-front occurs even in extreme acid conditions.

The morphology of transformed glass is determined by the ICDP-front. Monosilicic species are released at reaction front 2 and enter the local solution between reaction front 2 and 3 (see Fig. 6a). In acid conditions, the highly insoluble H_4SiO_4 is the dominating species. These species will trigger polymerization reactions at reaction front 3 where they form linear and randomly branched chains that invade the local solution. This leads to transformed glass with a homogeneous morphology. The term 'silica gel' can be used to describe this material, but that term is invalid for the silica material formed in alkaline conditions.

4.2. Transformation conditions in alkaline conditions (pH between 7 and 10)

From the observations, we can derive that transformed glass is not only formed in acid conditions but also in alkaline conditions. What we propose is that in an alkaline local solution transformed glass is formed according to Fig. 6b and that it consists of lamellae and silica nanoparticles. It is known that in acid conditions solutions of silicic acid endure polymerization reactions, forming a homogeneous gel

[29]. However, in alkaline solutions the same silicic species form spontaneously silica nanoparticles [22]. Also in the production of sol-gel silica films, a difference between acid and base-catalyzed films is reported resulting in respectively (1) a low porosity film composed of entangled linear or branched silica polymers and (2) porous film composed of silica nanoparticles [91, 92, 93, 94]. This suggests that the pH of the local solution plays a key role in the conversion of dissolved silica into amorphous silica at reaction front 3. It should be remarked that pH and pH fluctuations of the local solution can be different from that of the bulk solution.

The formation of silica nanoparticles does not explain the formation of lamellae by itself, meaning that other phenomena must play a role. We propose a transformation process that is governed by a cyclic pH evolution in the local solution and 2 regimes in which amorphous silica is formed at reaction front 3: (1) a regime at $\text{pH} < 9.8$ (i.e., pK_a of H_4SiO_4 [90]) where silica nanoparticles are formed at random positions (i.e., random loose packing) while the pH increases due to ion exchange, (2) a regime at $\text{pH} > 9.8$ where the particles are formed at positions with a somewhat higher ordering leading to a closed random packing and where the pH also continues to rise due to ion exchange but at a slower rate [15]. A sudden and spontaneous transition between a disordered packing and a more ordered packing occurs at the tipping point around $\text{pH} 9.8$. The tipping point is responsible for the closely conforming contours between the lamellae. At even higher pH, a chain reaction will be triggered that results in a sudden pH drop below 9.8. After that drop, the pH will gradually increase again. The 2 regimes, the tipping point distinguishing these regimes and the pH evolution as shown in Fig. 7 will be described in the following paragraphs. Observations have shown that the contrast between lamellae can be variable. This might be explained by the range in which the pH oscillates around the tipping point.

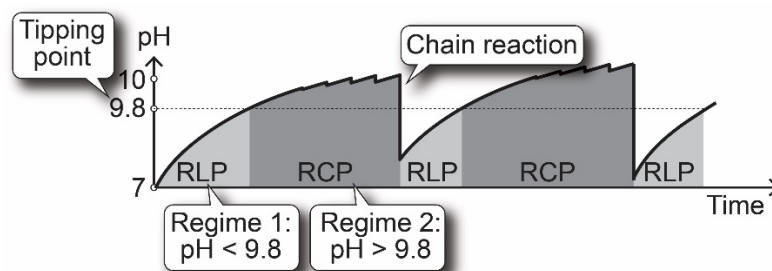


Fig. 7: The pH evolution in the local solution and the tipping point distinguishing the 2 regimes in which amorphous silica nanoparticles are formed with different packing.

a) Regime 1 at $\text{pH} < 9.8$ resulting in random loose packing (RLP)

The initial stage of this transformation process can be monitored with Atomic Force Microscopy. Glass with a typical medieval composition and other glass types in several atmospheric and liquid conditions show that the outer surface is covered by spherical particles with a size of 10-100 nm at random locations [91, 92, 93, 94]. Surface features (e.g., cracks) result locally in more rapid transformations [95]. The number of particles increase with time until the whole glass surface is covered [96, 97].

Once the glass surface is covered with silica nanoparticles, a local solution will be formed below the layer of particles. Within that solution, we propose that the nanoparticles are formed with a LaMer-like model where burst nucleation and particle growth alternate over time [98, 99]. At pH below 9.8, the nuclei are positioned at random positions leading to extensive disordered packing of silica nanoparticles (i.e., a random loose packing). The particle formation cycle is shown in Fig. 8. Nuclei formation and particle growth are described below:

- Nuclei formation:** When the monosilicic species in the local solution reaches oversaturation, nuclei will be formed at fixed positions on the surface of the previously formed nanoparticles (i.e., heterogeneous nucleation at reaction front 3) as is shown in Fig. 8. This results in some regularity of the position of nanoparticles in the direction vertical to the reaction front. Heterogeneous nucleation is more energy favourable than a homogeneous nucleation in the local solution. In addition, homogeneous nucleation will lead to mobile nuclei, which can migrate between the already formed nanoparticles. This should lead to lamellae with a much broader particle size distribution and will reduce the contrast between the consecutive lamellae, masking the formation of lamellae by structural patterning. This is not in agreement with the observations where contrasts between lamellae are easily observed with microscopic techniques. Due to a pKa of 9.8, the dominant monosilicic species in the local solution at pH < 9.8 is H_4SiO_4 while H_3SiO_4^- ions are only found in small amounts. The chemical reaction responsible for the nuclei formation and particle growth is a nucleophilic substitution reaction where H_3SiO_4^- ions act as the nucleophile and the silanol groups act as leaving group (see Fig. 9). The silanol groups of the nuclei are not acid enough and only a small fraction will release their protons. The nuclei are formed sequentially at random positions (see Fig. 8). The random positions of the nuclei results in a lamella with a random loose packing (RLP). Since nuclei are formed in a small planar zone at reaction front 3, each newly formed layer will be reasonable parallel to the previous one [100];
- Particle growth:** The continuous introduction of monosilicic species in the local solution allows the nuclei at fixed positions to grow. The silanol groups at the surface of the silica nanoparticles react with the minor amounts of H_3SiO_4^- ions that diffuses towards reaction front 3. Further particle growth keeps the concentration of dissolved monosilicic species below the point of oversaturation, inhibiting the formation of new nuclei. This means that particles of similar size are formed. The acidity of the silanol groups on the surface of the nanoparticles increases with the particle size from pKa = 9.5-10.7 down to 6.8 [90, 101]. When the particles are large enough, they will release their protons. In this regime, the release of protons has only a small effect on the increasing pH due to the dominant ion exchange process occurring at reaction front 1. Once the particle growth is hampered by a lack of open space (i.e., touch-and-stop model [102]), the particles will adhere by van der Waals' forces or perhaps by cementation around the contact points [103]. Since particle growth is hampered, the concentration of dissolved silica in the local solution rises. When a situation of oversaturation is reached, a new burst of nucleation occurs. The quasi-periodical LaMer-like mechanism explains the consecutive formation of silica nanoparticles in the same regime.

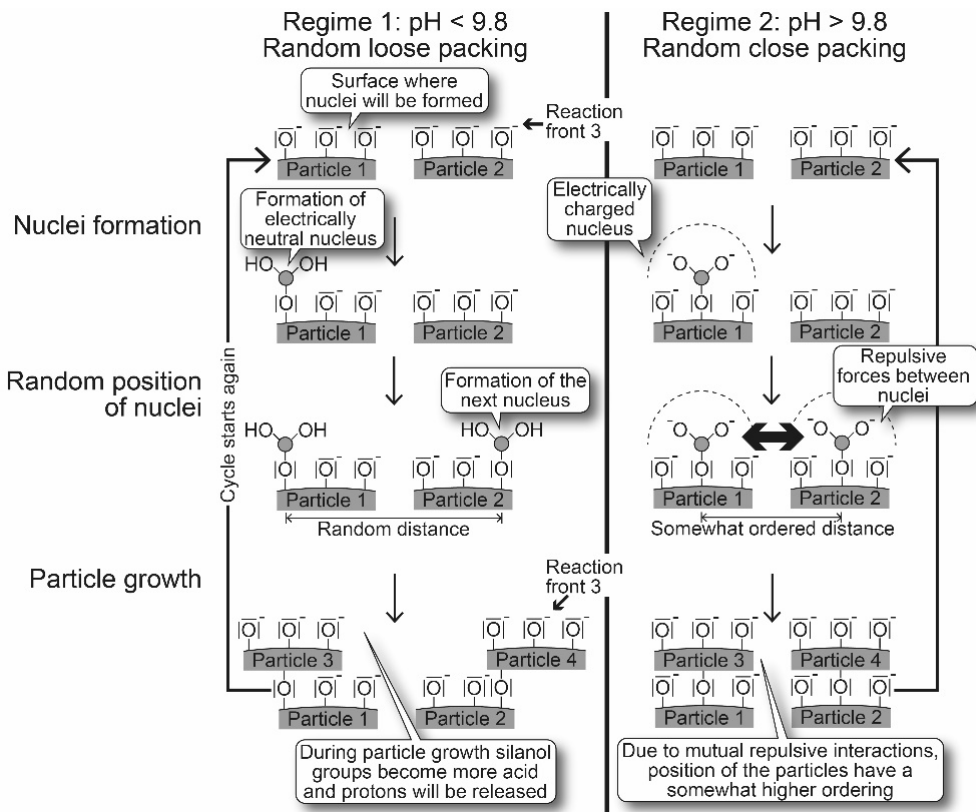


Fig. 8: Visual representation of the nucleation process and particle growth of silica nanoparticles at a microscopic level for a regime at pH < 9.8 and a regime at pH > 9.8, explaining the difference in packing of the silica nanoparticles.

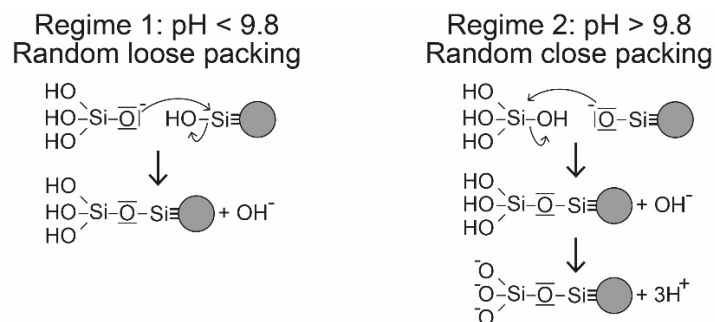


Fig. 9: Reaction mechanism at molecular level for a regime at pH < 9.8 and a regime at pH > 9.8

b) Regime 2 at pH > 9.8 resulting in random close packing (RCP)

The sudden transition from disorder (i.e., random loose packing) to higher order (i.e., random close packing) occurs when the increasing pH exceeds the pKa of silicic acid (at pH of 9.8). It is the ion exchange at reaction front 1 that causes the pH of the local solution (and of the bulk solution) to rise. The solubility of monosilicic species barely changes in the pH range 1-9, but increases rapidly above pH 9, because of the formation of silicic ions (see Fig. 10) [104]. At pH just above 9.8, the dominant monosilicic species becomes H_3SiO_4^- . It should be mentioned that the surfaces of the silica nanoparticles are negatively charged so that the H_3SiO_4^- ions are repelled by the already formed nanoparticles. The local solution is located inside a negatively charged cage and due to repelling forces negative ions cannot escape the local solution. The concentration of H_4SiO_4 remains constant for increasing pH (about 100-120 mg/L [105]). However, at elevated pH it will constitute a smaller fraction of the total dissolved silica content [106]. Also in this situation, the silica nanoparticles are formed by a LaMer-like model. The main difference is that for pH below the pKa, electrically neutral nuclei are

formed on negatively charged nanoparticle surfaces leading to a random loose packing (RLP), while at $\text{pH} > \text{pKa}$ the silanol groups of the nuclei are to a large extent deprotonated (see Fig. 8). As explained below, this will result in a random close packing (RCP).

- **Nuclei formation:** The nuclei formation is fairly similar to the one resulting in a random loose packing described earlier. The main difference at $\text{pH} > \text{pKa}$ is that a large fraction of the silanol groups of the nuclei will be deprotonated (see Fig. 8). This results in nuclei with elevated surface charge densities. In this situation, the deprotonated silanol groups act as nucleophile in the substitution reaction while an OH-group in the minor amounts of H_4SiO_4 contains the leaving group (see Fig. 9). The next nucleus being formed can be located anywhere but positions close to previously formed nuclei are somewhat disfavoured because of repulsive forces between the negatively charged nuclei. These repelling forces are weak and only result in some short-range order in the shell containing the nearest neighbouring nuclei. The positions of nuclei at larger distances are not affected by these forces and will appear random (long-range randomness). This form of ordering also occurs in the glass structure at the atomic level and explains the glassy state of the material [107]. This means that the location of a new nucleus depends on the positions of all the previously formed nuclei [108], resulting in some regularity in the positions of the nuclei. The equilibrated force balance results in an optimized distance distribution and thus in a somewhat higher ordering of the nuclei positions when compared to the situation at $\text{pH} < \text{pKa}$. This leads to a random close packing. The expected distance between nuclei should be fairly similar as the distance between adjacent, full grown particles.
- **Particle growth:** The concentration of dissolved monosilicic species is higher than the situation at pH below 9.8 and the abundant form of silica in solution is H_3SiO_4^- (see Fig. 10). Also in this situation, the particle growth will keep the concentration below oversaturation. Once the particles start to touch each other, particle growth slows down and dissolved silica will hardly be removed from the local solution. As a consequence, the continuous introduction of monosilicic species in the local solution due to dissolution at reaction front 2 causes a rise in that concentration and a situation of oversaturation will be reached again. New nuclei will be formed in the RCP-regime.

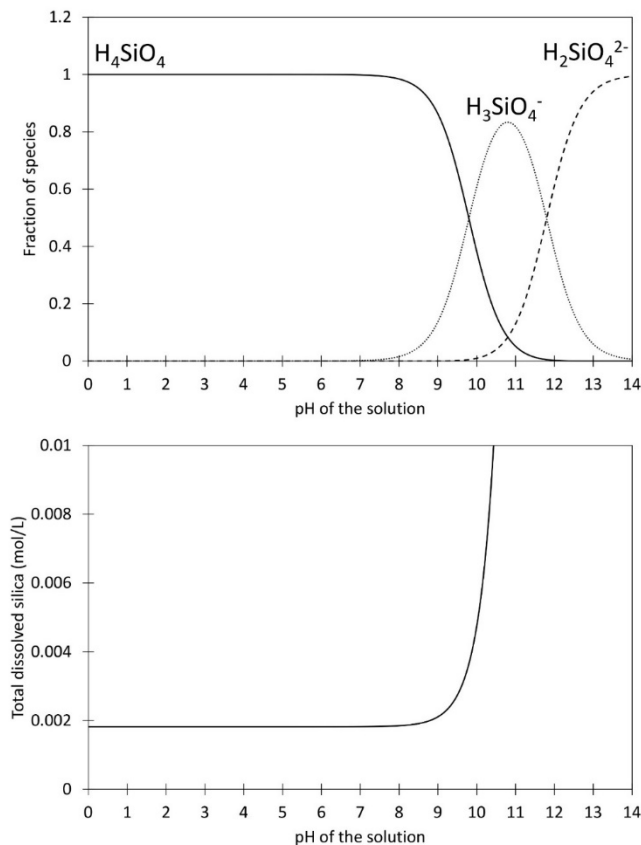


Fig. 10: The distribution of monosilicic species and the solubility of silica as a function of pH.

c) pH evolution in the local solution

The 2 regimes described in the previous paragraphs are connected to each other by the pH evolution in the local solution. The increasing pH caused by the ion exchange process at reaction front 1 explains the sudden transition from RLP to RCP when the tipping point of 9.8 is exceeded. The occurrence of alternating lamellae in transformed glass indicates that there is also an opposite transition from RCP to RLP. Therefore, there must exist a process responsible for a sudden drop in pH. The assumption of an oscillating pH is not new and was already suggested by others [54, 50]. This drop must be fast because the boundaries between RLP and RCP lamellae are sharp. Since this feedback loop is not observed in acid conditions, it must only occur in alkaline conditions. In addition, the drop in pH only occurs in the RCP-regime because it explains the transition from RCP to RLP. This suggests that it occurs at elevated pH. The section below describes that oscillation in detail.

- Steady increase in pH during the 2 regimes:** The ion exchange at reaction front 1 continuously removes protons from the local solution and from the bulk solution. This means that the pH gradually increases during the subsequent regimes of RLP and RCP but that the rate of proton absorption at reaction front 1 will gradually drop with increasing pH and even drop sharply between pH 9 and 11 [43]. Due to the small liquid volume of the local solution, the increase in pH will occur much faster in the local solution than for the bulk solution. When the pH of the local solution exceeds the pKa of silicic acid, the next nucleation burst will suddenly have a

random close packing (see Fig. 8). It explains the sharp contrast differences between subsequent lamellae.

- **Sudden drop in pH:** When the pH reaches a high alkalinity, the solubility of dissolved monosilicic species increases fast (see Fig. 10). Since higher amounts of monosilicic species can be dissolved in the local solution, the gap between healthy glass and transformed glass will steadily grow. Therefore, the volume of the local solution becomes larger. If oversaturation is reached, precipitation will occur following the reaction mechanism shown in Fig. 8. The newly formed silanol groups at the surface of the silica particles (4.6-4.9 silanol groups/nm² [101, 109]) will release their protons (see reaction mechanism of regime 2 in Fig. 9). When the local solution has a pH higher than 9 as is the case in the RCP-regime, the faint drop in pH severely reduces the solubility of silicic species (see Fig. 10). This makes that a part of the dissolved silicic species will be forced to precipitate in a RCP configuration. The silanol groups of these particles will release on their turn protons. This new drop in pH will not trigger a new precipitation when the original pH is not too high and when the total amount of dissolved monosilicic species is still small (i.e., see small pH drops in Fig. 7). However, when oversaturation is able to exist for some longer time so that the pH becomes more extreme and the total amount of dissolved species continues to rise a sudden drop in pH can trigger a chain reaction. At more extreme pH, the released protons cause a much larger drop in solubility (see Fig. 10) and the total amount of silica that is forced to precipitate is higher. This results in a larger number of newly formed silanol groups. The next drop in pH is also large because there are more protons that will be released. A new situation of oversaturation will be reached. The next wave of precipitation results in a further drop of the pH. Due to the sudden precipitation, the volume of the local solution becomes smaller and this pushes the drop in pH even more so that oversaturation is again reached. This chain reaction will stop at around pH 9 (i.e., the RLP regime) where a small drop in pH does not affect the solubility of dissolved silica in a substantial way. The strong nonlinearity of the solubility of silica where small changes in pH are amplified in extreme alkaline conditions explains the self-organisation. This chain reaction results in a severe pH drop in a short period of time, resulting in a sharp boundary between subsequent lamellae. It causes the pH to cross the tipping point so that the new nuclei will be formed in a RLP configuration. From that point onwards, the pH will gradually rise again due to the ion exchange process until the conditions are satisfied for a transition from RLP to RCP regimes and in a later stage for a next chain reaction resulting in a transition of RCP to RLP. The total drop in pH due to the chain reaction determines the contrast between consecutive lamellae because the ordering of the nuclei is pH dependent. The chain reaction only occurs at elevated pH and is for that reason not seen in acid conditions. For that reason, the formation of transformed glass in alkaline conditions is considered as a separate mechanism.

5. Conclusions

The experiments resulted in several critical observations that cannot be explained by the currently accepted degradation mechanisms of historical glass. The most important observation is that for identical glass, a different morphology of the internal structure of transformed glass formed under acid and alkaline conditions is obtained. This means that besides the well-known transformation mechanism in acid and extreme alkaline conditions an intermediate situation exists where a transformation layer is formed under alkaline conditions.. Depending of the pH of the solution, one of the 3 variants of the transformation process will be the dominant mechanism. An important

consequence of that observation is that accelerated degradation experiments in (extreme) acid solutions are not representative for samples that endured a much slower degradation in alkaline conditions. Transformed glass formed in alkaline conditions appear to contain Ca-rich inclusions. Such inclusions were not observed in transformed glass formed under acid conditions. Since this phenomenon is considered as a secondary process that occurs after the formation of transformed glass, it suggests that the occurrence of secondary processes is also pH-dependent. This means that the presence of inclusions might be used as an indicator for the pH at which transformed glass was formed.

The mechanism dominant at a pH between 7 and 10 is responsible for the formation of transformed glass in alkaline conditions. The process proposed explains how lamellae are formed. The ordering of the silica nanoparticles show sudden changes when a tipping point of pH = 9.8 is crossed. This results in consecutive lamellae with a random loose packing and a random close packing of silica nanoparticles. A mechanism is proposed that explains the oscillation of the pH in the local solution over time. The proposed transformation processes is able to describe the following observations:

- The sharp interface at the inner surface that cannot be explained with ion exchange only;
- The integration of several processes into a single mechanism such as ion exchange and the transformation of the silicate network into amorphous silica;
-
- The formation of lamellae in alkaline conditions only;
- The contrast between consecutive lamellae as a result of structural patterning;
- The variable contrast between subsequent lamellae depending on the range in which the pH oscillates;
- The regularity of positions of the silica nanoparticles parallel and perpendicular to the reaction front;
- The well resolved contours between lamellae due to a tipping point;
- Explanation of the self-organization due to the nonlinear behaviour of the silica solubility as a function of pH, the tipping point (i.e., pKa of silicic acid) and a chain reaction where small changes in pH are amplified.

Acknowledgements

The authors thanks prof. dr. Marc David and dr. Willemien Anaf for the numerous and fruitful discussions. The author is also grateful to dr. Kristel De Vis for her help in setting up the experiments.

References

- [1] N. Carmona, M. Villegas en J. Fernandez Navarro, „Characterization of an intermediate decay phenomenon of historical glasses,” *J. Mater. Sci.*, vol. 41, p. 2339–2346, 2006.
- [2] O. Schalm and W. Anaf, “Laminated altered layers in historical glass: density variations of silica nanoparticle random packings as explanation for the observed lamellae,” *J. Non-Cryst. Solids*, vol. 442, pp. 1-16, 2016.

- [3] O. Schalm, J. Caen en K. Janssens, „Homogeneity, Composition and Deterioration of Window Glass Fragments and Paint Layers from Two Seventeenth-Century Stained Glass Windows Created by Jan de Caumont (~1580–1659),” *Stud. Conserv.*, vol. 55, pp. 216-226, 2010.
- [4] O. Schalm, K. Proost, K. De Vis, S. Cagno, K. Janssens, F. Mees, P. Jacobs en J. Caen, „Manganese staining of archaeological glass: The characterization of Mn-rich inclusions in leached layers and a hypothesis of its formation,” *Archaeometry*, vol. 53, nr. 1, pp. 103-122, 2011.
- [5] I. Freestone, N. Meeks en A. Middleton, „Retention of phosphate in buried ceramics: an electron microbeam approach,” *Archaeometry*, vol. 27, nr. 2, pp. 161-177, 1985.
- [6] D. Brewster, “On the structure and optical phenomena of ancient decomposed glass,” *Trans. Roy. Soc. Edinb.*, vol. 23, p. 193–204, 1863.
- [7] M. Guillot, “Sur l’irisation du verre antique. Formation de strates de Liesegang dans le verre, au contact des solutions de bicarbonate, par précipitation rythmique de carbonate de calcium,” *Comptes rendus de l’Académie des sciences*, vol. 198, p. 2093–2095, 1934.
- [8] H. Roemich, S. Gerlach, P. Mottner, F. Mees, P. Jacobs, D. van Dyck and T. Doménech-Carbó, “Results from burial experiments with simulated medieval glasses,” *Mat. Res. Soc. Symp. Proc.*, vol. 757, pp. II2.3.1-II2.3.11, 2003.
- [9] R. Brill and H. Hood, “A new method for dating ancient glass,” *Nature*, vol. 189, pp. 12-14, 1961.
- [10] G. Shaw, “Weathered crusts on ancient glass,” *New Sci.*, vol. 29, pp. 290-291, 1965.
- [11] R. Newton, „The enigma of the layered crusts on some weathered glasses, a chronological account of the investigations,” *Archaeometry*, vol. 13, nr. 1, pp. 1-9, 1971.
- [12] G. Cox en B. Ford, „The corrosion of glass on the sea bed,” *J. Mater. Sci.*, vol. 24, pp. 3146-3153, 1989.
- [13] A. Silvestri, C. Viti, G. Molin and G. Salviulo, “From micro- to nano-arrangement: alteration products in archaeological glass from marine and land-based environments,” *Proceedings of the 37th International Symposium on Archaeometry*, p. 383–385, 2011.
- [14] M. Melcher en M. Schreiner, „Glass degradation by liquids and atmospheric agents,” in *Modern methods for analysing archaeological and historical glass*, West Sussex, John Wiley & Sons, 2013, p. 609.
- [15] R. Douglas and T. El-Shamy, “Reactions of glasses with aqueous solutions,” *J. Am. Ceram. Soc.*, vol. 50, no. 1, pp. 1-9, 1967.

- [16] Y. Moriya, „Factors affecting the hydration of silicate glass,” *Bull. Inst. Chem. Res., Kyoto Univ.*, vol. 59, nr. 3, pp. 212-223, 1981.
- [17] G. Woisetschläger, M. Dutz, S. Paul en M. Schreiner, „Weathering Phenomena on Naturally Weathered Potash-Lime-Silica-Glass with Medieval Composition Studied by Secondary Electron Microscopy and Energy Dispersive Microanalysis,” *Microchim. Acta*, vol. 135, pp. 121-130, 2000.
- [18] N. Carmona, M. Villegas en J. Fernández Navarro, „Corrosion behaviour of R2O-CaO-SiO2 glasses submitted to accelerated weathering,” *J. Eur. Ceram. Soc.*, vol. 25, pp. 903-910, 2005.
- [19] M. Melcher, M. Schreiner en K. Kreislova, „Artificial weathering of model glasses with medieval compositions: An empirical study on the influence of particulates,” *Phys. Chem. Glasses-B*, vol. 49, nr. 6, pp. 346-356, 2008.
- [20] T. palomar, „Chemical composition and alteration processes of glasses from the cathedral of León (Spain),” *Bol. Soc. Esp. Ceram. V.*, vol. 57, nr. 3, pp. 101-111, 2018.
- [21] R. K. Iler, *The Chemistry of silica: Solubility, polymerization, colloid and surface properties and biochemistry of silica*, New York: Wiley, 1979.
- [22] P. Bird, „Colloidal solutions of inorganic oxides”. USA Patent 2,244,325, 3 June 1941.
- [23] M. Bechtold en O. Snyder, „Chemical processes and composition”. USA Patent 2,574,902, 13 November 1951.
- [24] J. Rule, „Process of making stable silica sols and resulting composition”. USA Patent 2,577,485, 4 December 1951.
- [25] R. Marotta, „Process for preparing silica aquasols”. USA Patent 3,374,180, 19 March 1968.
- [26] W. Albrecht, „Silica sols containing large particle size silica”. USA Patent 3,947,376, 30 March 1976.
- [27] U. Brekau, A. Nickel, H. Block, M. H.H., S. P., P. Schober en W. Ludovici, „Process for the production and concentration of silica sols”. USA Patent 5,458,812, 17 October 1995.
- [28] J. Jones, J. Sanders en E. Segnit, „Structure of opal,” *Nature*, vol. 204, pp. 990-991, 1964.
- [29] R. Iler, „Formation of precious opal,” *Nature*, vol. 207, p. 472-473, 1965.
- [30] J. Jones, J. Biddle en E. Segnit, „opal genesis,” *Nature*, vol. 210, pp. 1353-1354, 1966.
- [31] O. Velez en A. Lenhoff, „Colloidal crystals as templates for porous materials,” *Curr. Opin. Colloid In.*, vol. 5, pp. 56-63, 2000.

- [32] W. Geilman, „Beiträge zur Kenntnis alter Gläser IV: Die Zersetzung der Gläser im Bodem,” *Glasstechn. Ber.*, vol. 4, pp. 145-168, 1956.
- [33] R. Newton, „Some further observation on the weathering crusts of ancient glass,” *Glass Techn.*, vol. 10, nr. 2, pp. 40-42, 1969.
- [34] R. Newton, „Stereoscan views of weathering layers on a piece of ancient glass,” *Glass Techn.*, vol. 13, nr. 2, pp. 54-56, 1972.
- [35] J. Sterpenich en G. Libourel, „Using stained glass windows to understand the durability of toxic waste matrices,” *Chem. Geol.*, vol. 175, pp. 181-193, 2001.
- [36] J. Sterpenich, „Cristallochimie des produits d'altération des vitraux médiévaux: application au vieillissement des déchets vitrifiés,” *Bull. Eng. Geol. Env.*, vol. 61, pp. 179-193, 2002.
- [37] B. Dal Bianco, R. Bertocello, L. Milanese en S. Barison, „Glass corrosion across the Alps: A surface study of chemical corrosion of glasses found in marine and land-based environments,” *Archaeometry*, vol. 47, nr. 2, pp. 351-360, 2005.
- [38] A. Silvestri, G. Molin en Salviulo, „Archaeological glass alteration products in marine and land-based environments: morphological, chemical and microtextural characterization,” *J. Non-Cryst. Solids*, vol. 351, nr. 16-17, pp. 1338-1349, 2005.
- [39] M. Doménech-Carboó, L. Doménech-Carboó, L. Osete-Cortina en M. Sauri-Peris, „A study on corrosion processes of archaeological glass from the Valencian region (Spain) and its consolidation treatment,” *Microchim. Acta*, nr. 154, pp. 123-142, 2006.
- [40] G. Libourel, A. Verney-Carron, A. Morlok, S. Gin, J. Sterpenich, A. Michelin, D. Neff en P. Dillmann, „The use of natural and archeological analogues for understanding the long-term behavior of nuclear glasses,” *C. R. Geosci.*, vol. 343, pp. 237-245, 2011.
- [41] T. Lombardo, L. Gentaz, A. Verney-Carron, A. Chabas, C. Loisel, D. Neff en E. Leroy, „Characterization of complex alteration layers in medieval glasses,” *Corr. Sci.*, vol. 72, pp. 10-19, 2013.
- [42] C. Lenting, O. Plümper, M. Kilburn, P. Guagliardo, M. Klinkenberg and T. Geisler, „Towards a unifying mechanistic model for silicate glass corrosion,” *npj Mater. Degrad.*, vol. 2, no. 28, 2018.
- [43] B. Bunker, „Molecular mechanisms for corrosion of silica and silicate glasses,” *J. Non-Cryst. Solid.*, vol. 179, pp. 300-308, 1994.
- [44] A. Verney-Carron, L. Sessegolo, M. Saheb, N. Valle, P. Ausset, R. Losno, D. Mangin, T. Lombardo, A. Chabas en C. Loisel, „Understanding the mechanisms of Si-K-Ca glass alteration using silicon isotopes,” *Geochim. Cosmochim. Acta*, vol. 203, pp. 404-421, 2017.

- [45] I. Koch, „Petri Nets – A mathematical formalism to analyze chemical reaction networks,” *Mol. Inf.*, vol. 29, pp. 838-843, 2010.
- [46] L. Hench, „Characterization of glass corrosion and durability,” *J. Non-Cryst. Solids*, vol. 19, pp. 27-39, 1975.
- [47] D. Clark, M. Dilmore, E. Ethridge en L. Hench, „Aqueous Corrosion of Soda-Silica and Soda-Lime-Silica Glass,” *J. Am. Ceram. Soc.*, vol. 59, nr. 1-2, pp. 62-65, 1976.
- [48] L. Hench en D. Clark, „Physical chemistry of glass surfaces,” *J. Non-Cryst. Solids*, vol. 28, pp. 83-105, 1978.
- [49] C. Cailleteau, F. Devreux, O. Spalla, F. Angeli en S. Gin, „Why do certain glasses with a high dissolution rate undergo a low degree of corrosion?,” *J. Phys. Chem. C*, vol. 115, pp. 5846-5855, 2011.
- [50] L. Dohmen, C. Lenting, R. O. Fonseca, T. Nagel, A. Heuser and T. Geisler, “Pattern formation in silicate glass corrosion zones,” *Int. J. Appl. Glass Sci.*, vol. 4, no. 4, pp. 357-370, 2013.
- [51] W. Geilmann, “Microscopic inspection of glass,” *Zeiss Werkzeitschrift (English edition)*, vol. 38, pp. 94-96, 1960.
- [52] C. V. Raman en V. S. Rajagopalan, „The structure and optical characters of iridescent glass,” *Proc. Indian Acad. Sci.*, vol. A9, p. 371–381, 1939.
- [53] C. V. Raman en V. S. Rajagopalan, „Colors of stratified media — I. ancient decomposed glass,” *Proc. Indian Acad. Sci.*, vol. A11, p. 469–482, 1940.
- [54] G. Cox and B. Ford, “The long-term corrosion of glass by ground water,” *J. mater. Sci.*, vol. 28, pp. 5637-5647, 1993.
- [55] T. Geisler, A. Janssen, D. Scheiter, T. Stephan, J. Berndt and A. Putnis, “Aqueous corrosion of borosilicate glass under acidic conditions: A new corrosion mechanism,” *J. Non-Cryst. Solids*, vol. 356, pp. 1458-1465, 2010.
- [56] H. E. King, O. Plümper, T. Geisler and A. Putnis, “Experimental investigations into the silicification of olivine: Implications for the reaction mechanism and acid neutralization,” *Am. Mineral.*, vol. 96, pp. 1503-1511, 2011.
- [57] R. Hellmann, R. Wirth, D. Daval, J.-P. Barnes, J.-M. Penisson, D. Tisserand, T. Epicier, B. Florin and R. L. Hervig, “Unifying natural and laboratory chemical weathering with interfacial dissolution-precipitation: A study based on the nanometer-scale chemistry of fluid-silicate interfaces,” *Chem. Geol.*, Vols. 294-295, pp. 203-216, 2012.

- [58] T. Geisler, T. Nagel, M. R. Kilburn, A. Janssen, J. P. Icenhower, R. O. Fonseca, M. Grange and A. A. Nemchin, "The mechanism of borosilicate glass corrosion revisited," *Geochim. Cosmochim. Ac.*, vol. 158, pp. 112-129, 2015.
- [59] T. Geisler, L. Dohmen, C. Lenting and M. B. Fritsche, "Real-time in situ observations of reaction and transport phenomena during silicate glass corrosion by fluid-cell Raman spectroscopy," *Nat. Mater.*, vol. 18, p. 342–348, 2019.
- [60] Y. Wang, C. Jove-Colon, C. Lenting, J. Icenhower en L. Huhman, „Morphological instability of aqueous dissolution of silicate glasses and minerals," *npj Mater. Degrad.*, vol. 27, nr. 2, 2018.
- [61] O. Schalm, D. Calluwé, H. Wouters, K. Janssens, F. Verhaeghe en P. M., „Chemical composition and deterioration of glass excavated in the 15th–16th century fishermen town of Raversijde (Belgium)," *Spectrochim. Acta B*, vol. 59, p. 1647– 1656, 2004.
- [62] O. Schalm, K. Janssens, H. Wouters en D. Calluwé, „Composition of 12–18th century window glass in Belgium:Non-figurative windows in secular buildings and stained-glass windows in religious buildings," *Spectrochim. Acta B*, vol. 62, p. 663–668, 2007.
- [63] M. De Bardi en R. S. M. Wiesinger, „Leaching studies of potash–lime–silica glass with medieval composition by IRRAS," *J. Non-Cryst. Sol.*, vol. 360, pp. 57-63, 2013.
- [64] M. Gulmini, M. Pace, G. Ivaldi, M. Ponzi en P. Mirti, „Morphological and chemical characterization of weathering products on buried Sasanian glass from central Iraq," *J. Non-Cryst. Solids*, nr. 355, pp. 1613-1621, 2009.
- [65] M. Melcher en M. Schreiner, „Statistical evaluation of potash-lime-silica glass weathering," *Anal. Bioanal. Chem.*, vol. 379, p. 628–639, 2004.
- [66] M. Melcher en M. Schreiner, „Leaching studies on naturally weathered potash-lime-silica glasses," *J. Non-Cryst. Solids*, vol. 352, p. 368–379, 2006.
- [67] M. Melcher en M. Schreiner, „Quantification of the influence of atmospheric pollution on the weathering of low-durability potash-lime-silica glasses," *Pollut. Atmos.*, vol. 49, pp. 13-22, 2007.
- [68] M. Melcher, R. Wiesinger en M. Schreiner, „Degradation of glass artifacts: Application of modern surface analytical techniques," *Acc. Chem. Res.*, vol. 43, nr. 6, p. 916–926, 2010.
- [69] R. Doremus, „Diffusion of water in silica glass," *J. Mater. Res.*, vol. 10, nr. 9, pp. 2379-2389, 1995.
- [70] R. Doremus, „Diffusion of water in rhyolite glass: diffusion-reaction model," *J. Non-Cryst. Solids*, vol. 261, pp. 101-107, 2000.

- [71] J. Sterpenich en G. Libourel, „Water diffusion in silicate glasses under natural weathering conditions: evidence from buried medieval stained glasses,” *J. Non-Cryst. Sol.*, vol. 352, pp. 5446-5451, 2006.
- [72] L. De Ferri, P. Lottici en G. Vezzalini, „Characterization of alteration phases on potash-lime-silica glass,” *Corros. Sci.*, vol. 80, pp. 434-441, 2014.
- [73] L. Sessegolo, A. Verney-Carron, P. Ausset, M. Saheb and A. Chabas, „Effect of the surface roughness on medieval-type glass alteration in aqueous medium,” *J. Non-Cryst. Solids*, vol. 505, pp. 260-271, 2019.
- [74] C. Jantzen, K. Brown en J. Pickett, „Durable glass for thousands of years,” *Int. J. Appl. Glass Sci.*, vol. 1, nr. 1, pp. 38-62, 2010.
- [75] M. Thomas, „The effect of supplementary cementing materials on alkali-silica reaction: A review,” *Cement Concrete Res.*, vol. 41, p. 1224–1231, 2011.
- [76] F. Rajabipour, E. Giannini, C. Dunant, J. Ideker en M. Thomas, „Alkali–silica reaction: Current understanding of the reaction mechanisms and the knowledge gaps,” *Cement Concrete Res.*, vol. 76, p. 130–146, 2015.
- [77] R. Figueira, S. R., L. Coelho, M. Azenha, d. A. J.M., P. Jorge en S. C.J.R., „Alkali-silica reaction in concrete: Mechanisms, mitigation and test methods,” *Constr. Build. Mater.*, vol. 222, p. 903–931, 2019.
- [78] E. Prodan, „Reactions in solid state: localized and delocalized,” *J. Thermal Anal.*, vol. 36, pp. 1963-1972, 1990.
- [79] T. El Shamy, „Decomposition of silicate glasses in alkaline solutions,” *Nature*, vol. 266, pp. 704-706, 1977.
- [80] W. Müller, M. Torge en K. Adam, „Primary stabilization factor of the corrosion of historical glasses: the gel layer,” *Glastech. Ber. Glass Sci. Technol.*, vol. 68, pp. 285-292, 1995.
- [81] R. Doremus, Y. L. W. Mehrotra en C. Burman, „Reaction of water with glass: influence of a transformed surface layer,” *J. Mater. Sci.*, vol. 18, pp. 612-622, 1983.
- [82] W. Lanford, „Ion beam analysis of glass surfaces: dating, authentication and conservation,” *Nucl. Instrum. Meth. B*, vol. 14, nr. 1, pp. 123-126, 1986.
- [83] K. Schnatter, R. Doremus en W. Lanford, „Hydrogen analysis of soda-lime silicate glass,” *J. Non-Cryst. Solids*, vol. 102, pp. 11-18, 1988.
- [84] Z. Bocksay, G. Bouquet en S. Dobos, „Diffusion processes in the surface layer of glass,” *Phys. Chem. Glass.*, vol. 8, nr. 4, pp. 140-144, 1967.

- [85] F. Ernsberger, „The role of molecular water in the diffusive transport of protons in glasses,” *Phys. Chem. Glass*, vol. 21, nr. 4, pp. 146-149, 1980.
- [86] M. De Bardi, H. Hutter en M. Schreiner, „ToF-SIMS analysis for leaching studies of potash–lime–silica glass,” *Appl. Surf. Sci.*, vol. 282, nr. 1, pp. 195-201, 2013.
- [87] P. Colomban, M. Etcheverry, A. M., M. Bounichou en A. Tourni, „Raman identification of ancient stained glasses and their degree of deterioration,” *J. Raman Spectroc.*, vol. 37, p. 614–626, 2006.
- [88] L. De Ferri, D. Bersani, P. Colomban, P. Lottici en G. V. G. Simon, „Raman study of model glass with medieval compositions: artificial weathering and comparison with ancient samples,” *J. Raman Spectrosc.*, vol. 43, nr. 11, pp. 1817-1823, 2012.
- [89] L. Hench, R. Newton en S. Bernstein, „Use of infrared spectroscopy in analysis of durability of medieval glasses, with some comments on conservation procedures,” *Glass Techn.*, vol. 20, nr. 4, pp. 144-148, 1979.
- [90] M. Lynch, F. D.C. en D. Clark, „Use of FTIR reflectance spectroscopy to monitor corrosion mechanisms on glass surfaces,” *J. Non-Cryst. Solids*, vol. 353, pp. 2667-2674, 2007.
- [91] J. Hong, H. Kim en H. Park, „The effect of sol viscosity on the sol-gel derived low density SiO₂ xerogel film for intermetal dielectric application,” *Thin Solid Films*, vol. 332, pp. 449-454, 1998.
- [92] G. Wu, J. Wang, J. Shen, Y. T., Q. Zhang, B. Zhou, Z. Deng, B. Fan, D. Zhou en F. Zhang, „A novel route to control refractive index of sol-gel derived nano-porous silica films used as broadband antireflective coatings,” *Mater. Sci. Eng.*, vol. B78, pp. 135-139, 2000.
- [93] Y. Xiao, J. Shen, Z. Xie, B. Zhou en G. Wu, „Microstructure control of nanoporous silica thin film prepared by sol-gel process,” *J. Mater. Sci. Technol.*, vol. 23, nr. 4, pp. 504-508, 2007.
- [94] H. Ye, X. Zhang, Y. Zhang, L. Ye, B. Xiao, H. Lv en B. Jiang, „Preparation of antireflective coatings with high transmittance and enhanced abrasion-resistance by a base/acid two-step catalyzed sol-gel process,” *Sol. Energ. Mat. Sol. C.*, vol. 95, pp. 2347-2351, 2011.
- [95] D. Belton, O. Deschaume en C. Perry, „An overview of the fundamentals of the chemistry of silica with relevance to biosilicification and technological advances,” *FEBS*, vol. 279, nr. 10, pp. 1710-1720, 2012.
- [96] I. Schmitz, T. Prohaska, M. Schreiner and M. Grassbauer, „Investigation of corrosion processes on cleavage edges of potash-lime-silica glasses by atomic force microscopy,” *Fresenius J. Anal. Chem.*, vol. 353, pp. 666-669, 1995.
- [97] I. Schmitz, M. Schreiner, G. Friedbacher and M. Grassbauer, „Phase imaging as an extension to tapping mode AFM for the identification of material properties on humidity-sensitive surfaces,” *Appl. Surf. Sci.*, vol. 115, pp. 190-198, 1997.

- [98] N. Donzel, S. Gin, F. Augereau and M. Ramonda, "Study of gel development during SON68 glass alteration using atomic force microscopy: Comparison with two simplified glasses," *J. Nucl. Mater.*, vol. 317, pp. 83-92, 2003.
- [99] N. Carmona, A. Kowal, J.-M. Rincon and M.-A. Villegas, "AFM assessments of the surface nano/microstructure on chemically damaged historical and model glasses," *Mater. Chem. Phys.*, vol. 119, pp. 254-260, 2010.
- [100] S. Henderson, J. Castle and Z. P., "The SPM and XPS characterization of the corrosion resistance of glasses," in *Advances in the Characterization of Ceramics*, R. Freer, B. Derby and B. Lewis, Red., British Ceramics Proc., 1997, pp. 54-66.
- [101] M. Schreiner, G. Woisetschläger, I. Schmitz and M. Wadsak, "Characterization of surface layers formed under natural environmental conditions on medieval stained glass and ancient copper alloys using SEM, SIMS and atomic force microscopy," *J. Anal. At. Spectrom.*, vol. 14, pp. 395-403, 1999.
- [102] D. R. Tadjiev and R. J. Hand, "Surface hydration and nanoindentation of silicate glasses," *J. Non-Cryst. Solids*, vol. 356, pp. 102-108, 2010.
- [103] V. K. LaMer and R. H. Dinegar, "Theory, production and mechanism of formation of monodispersed hydrosols," *J. Am. Chem. Soc.*, vol. 72, no. 11, pp. 4847-4854, 1950.
- [104] C. B. Whitehead, S. Ozkar and R. G. Finke, "LaMer's 1950 model for particle formation of instantaneous nucleation and diffusion-controlled growth: A historical look at the model's origins, assumptions, equations, and underlying sulfur sol formation kinetics data," *Chem. Mater.*, vol. 31, no. 18, p. 7116-7132, 2019.
- [105] R. Newton and S. G., "Another unsolved problem concerning weathering layers," *Glass Techn.*, vol. 29, nr. 2, pp. 78-79, 1988.
- [106] S. Patwardhan, F. Emami, R. Berry, S. Jones, R. Naik, O. Deschaume, H. Heinz and P. C.C., "Chemistry of aqueous silica nanoparticle surfaces and the mechanism of selective peptide adsorption," *J. Am. Chem. Soc.*, vol. 134, pp. 6244-6256, 2012.
- [107] Y. A. Andrienko, "Pattern formation by growing droplets: The touch-and-stop model of growth," *J. Stat. Phys.*, vol. 75, no. 3, pp. 507-523, 1994.
- [108] D. Norris, E. Arlinghaus, L. Meng, R. Heiny and L. Scriven, "Opaline photonic crystals: How does self-assembly work?," *Adv. Mater.*, vol. 16, nr. 16, pp. 1393-1399, 2004.
- [109] T. Tarutani, "Polymerization of silicic acid: A review," *Anal. Sci.*, vol. 5, pp. 245-252, 1989.
- [110] M. Dietzel, "Dissolution of silicates and the stability of polysilicic acid," *Geochim. Cosmochim. Ac.*, vol. 64, nr. 19, pp. 3275-3281, 2000.

- [111] G. Alexander, W. Heston en R. Iler, „The solubility of amorphous silica in water,” *J. Phys. Chem.*, vol. 58, nr. 6, p. 453–455, 1954.
- [112] P. Gaskell, M. Eckersley, A. Barnes en Chieux, „Medium-range order in the cation distribution of a calcium silicate glass,” *Nature*, vol. 350, pp. 675-677, 1991.
- [113] S. Ahn and S. J. Lee, “Collective ordering of microscale matters in natural analogy,” *Sci. Rep.*, vol. 5, no. 10790, 2015.
- [114] L. Zhuravlev, „The surface chemistry of amorphous silica. Zhuravlev model,” *Colloid Surface A*, vol. 173, pp. 1-38, 2000.